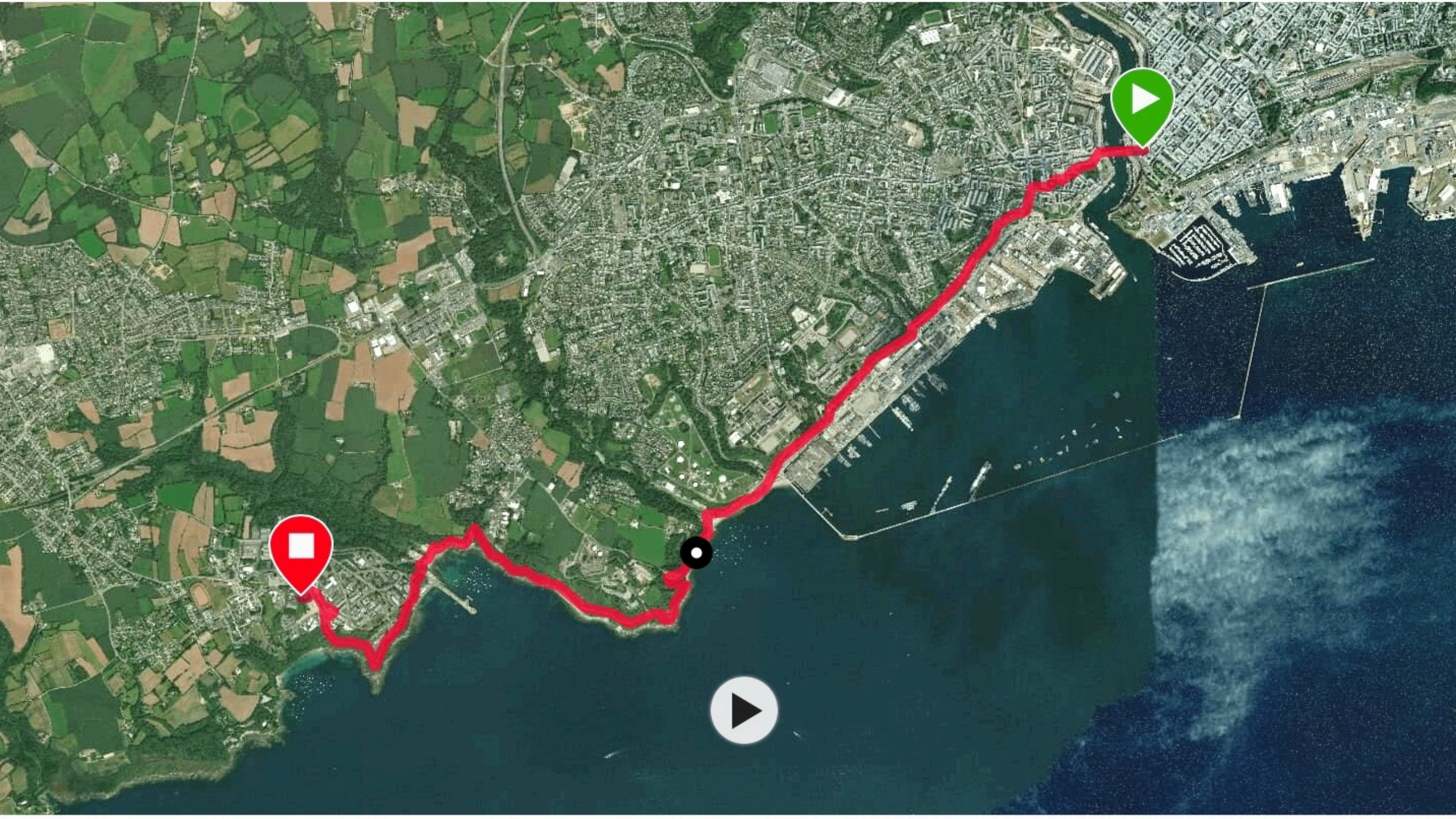


# **Towards improved estimates of upper ocean energetics: Science motivation for simultaneous measurements of ocean surface vector winds and currents**

Dimitris Menemenlis (Jet Propulsion Laboratory)  
Doppler Oceanography from Space  
10-12 October 2018 Brest (France)

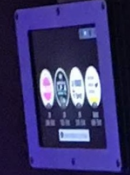
- 1. Global internal-wave-admitting ocean circulation + tides simulation**
- 2. Evaluation of simulation results vs observations**
- 3. Some upper ocean applications**
- 4. Future directions and concluding remarks**

**Model development:** C. Hill, C. Henze, B. Nelson, B. Ciotti, G. Forget, A. Nguyen, A. Chaudhuri, ...  
**Science applications:** P. Klein, H. Torres, J. Wang, Z. Su, A. Thompson, M. Flexas, A. Stewart, M. Losch, N. Hutter, F. Ardhuin, A. Ponte, C. Peureux, X. Yu, C. Wunsch, Z. Liu, K. Drushka, L. Rainville, A. Savage, C. Rocha, J. Ansong, B. Arbic, B. Qiu, T. Farrar, T. Chereskin, S. Gille, ...





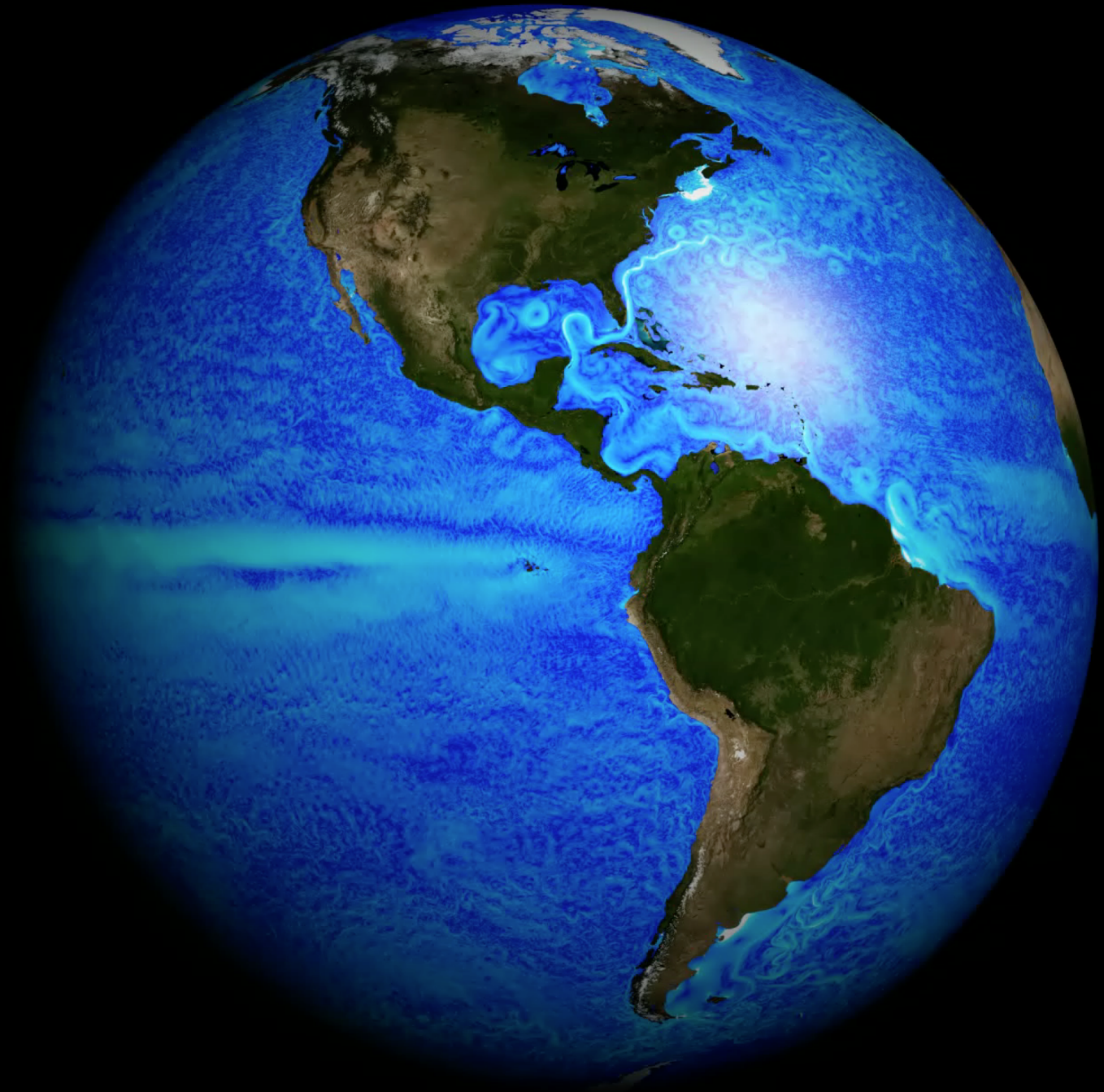
UN PETIT CHOUX ?  
Plus accompagner vos plats  
de viande ou de poisson  
4€  
Sans alcool, version de poche  
à emporter  
Une pâtisserie parfaite

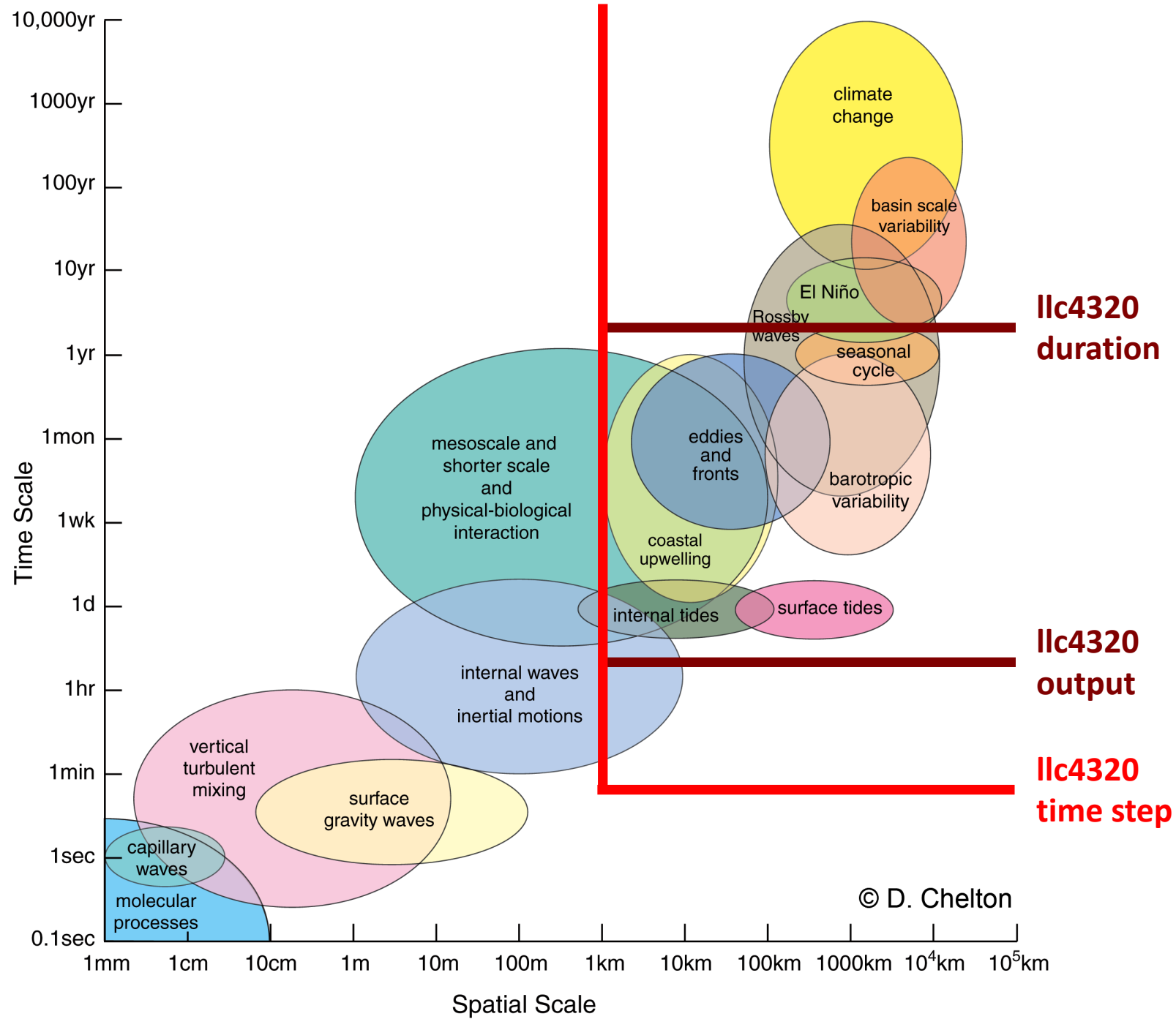


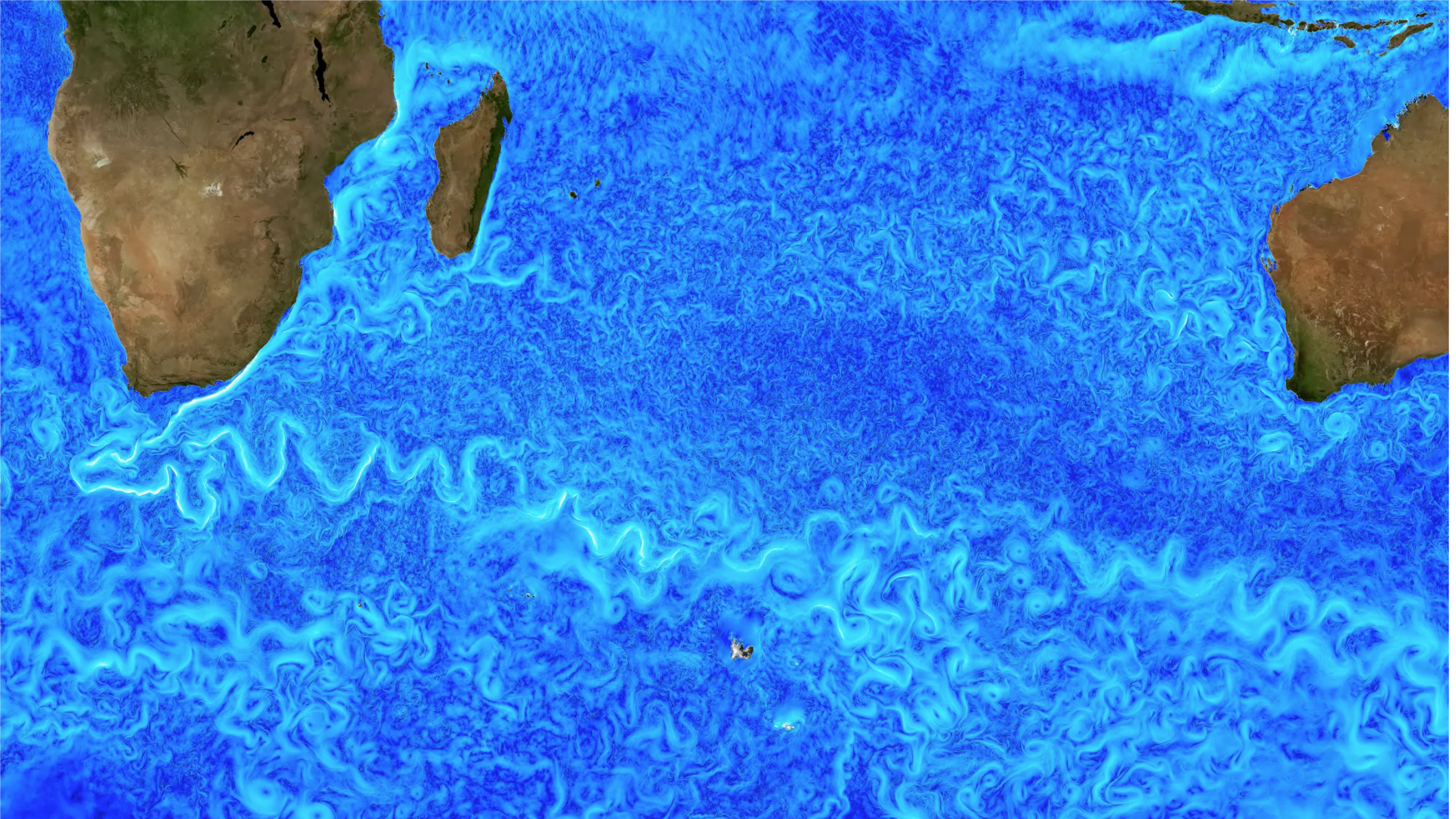
BALAST  
WORMCORE & FREAKS  
HASSAN  
PARTOUT / PARTOUT  
-01 NOV  
ESPACE LEO FERR  
21H/5€

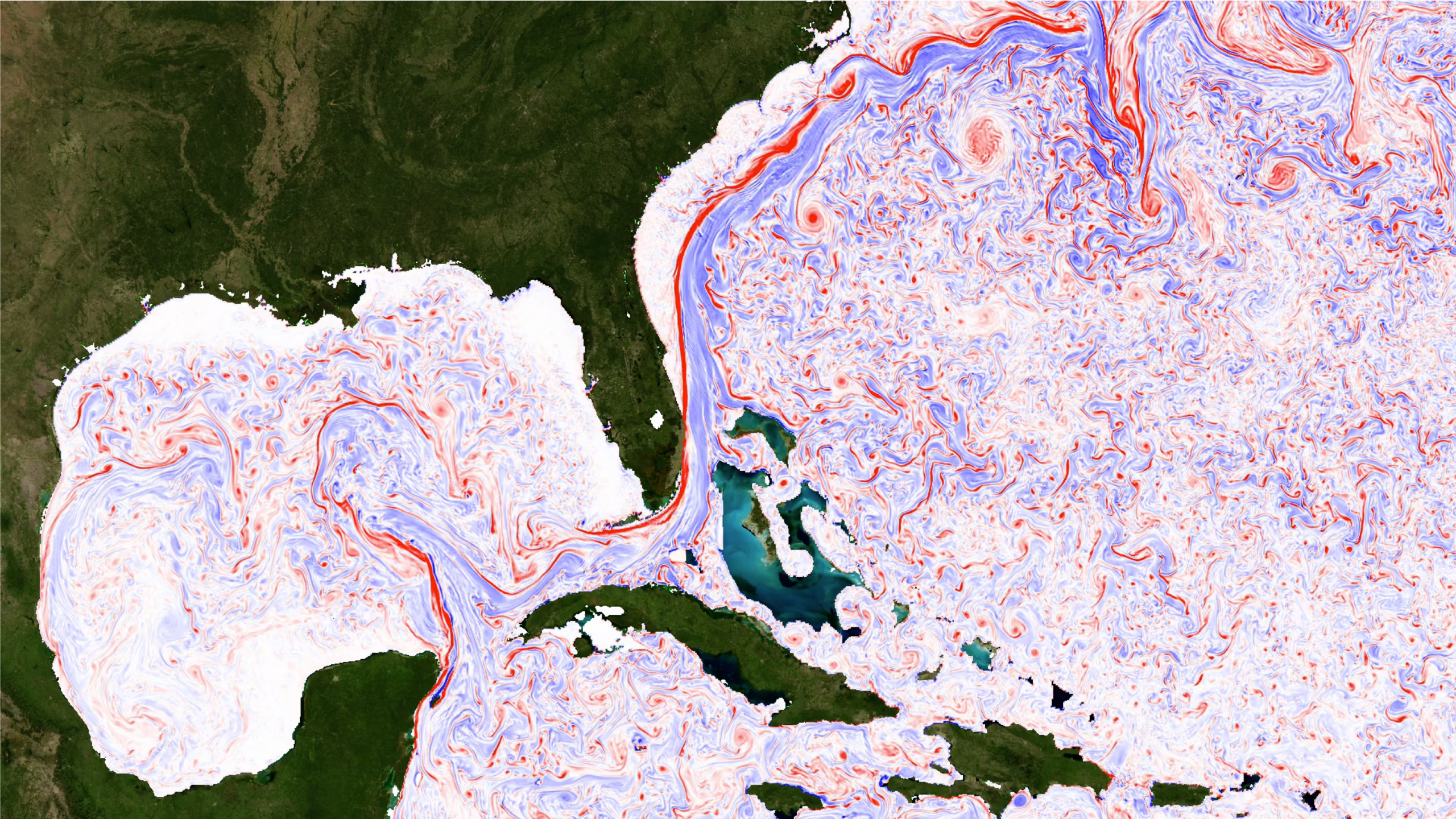


Global internal-wave-admitting ocean  
circulation + tides simulation











Cracks in the ice

# Sea Ice

Concentration (Opacity)  
and Thickness (Shadowing)

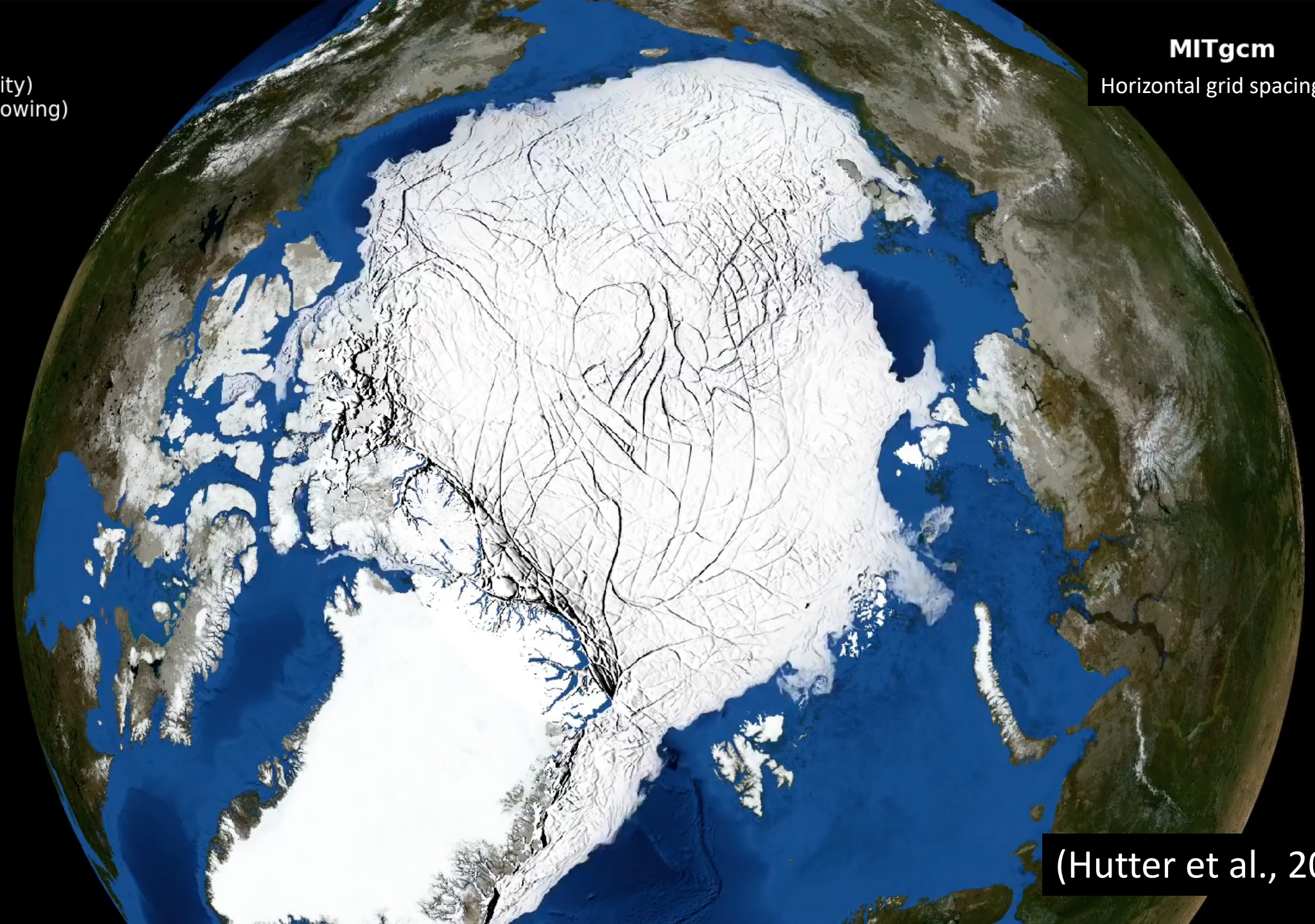
MITgcm

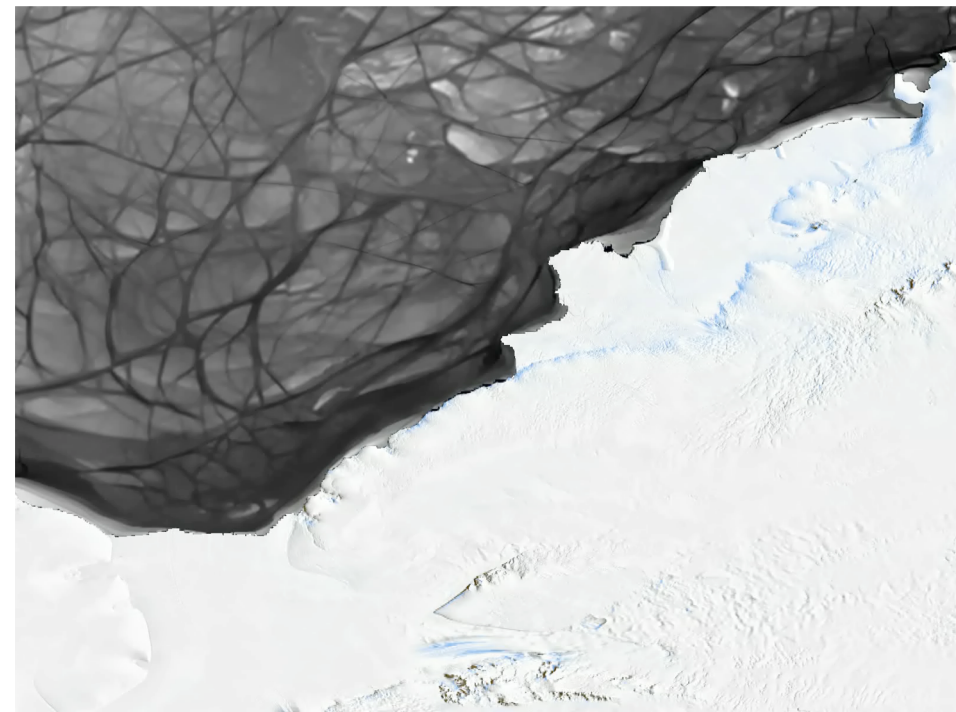
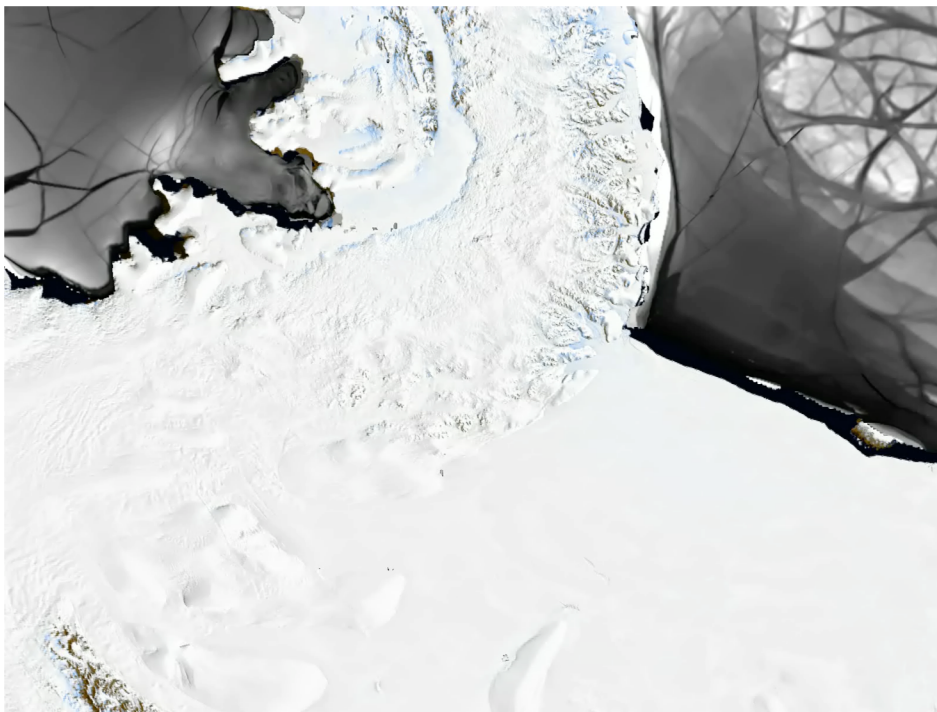
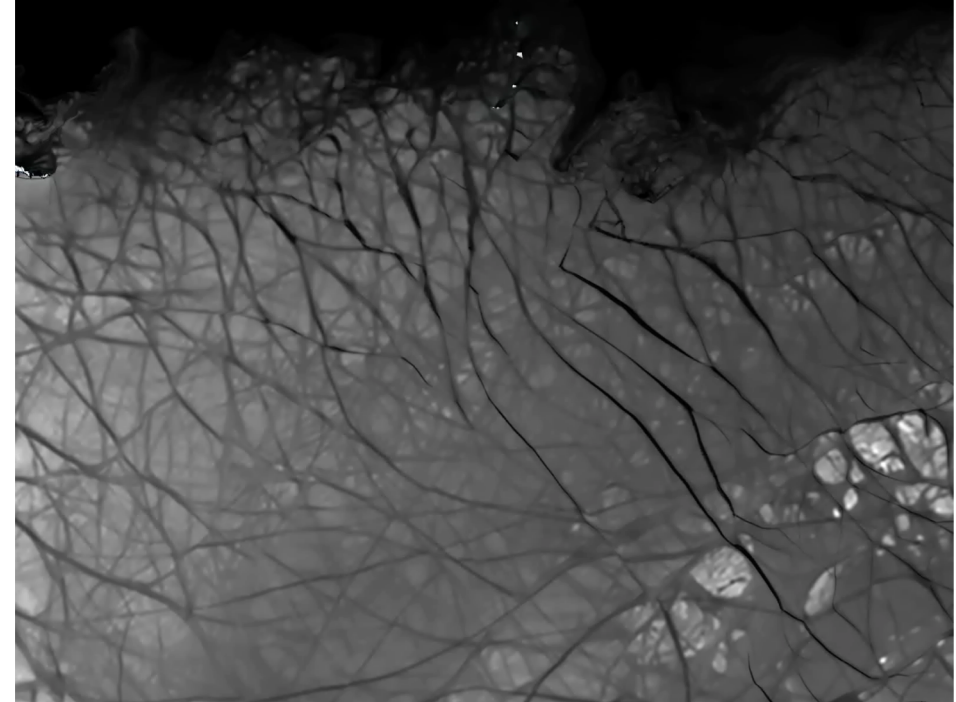
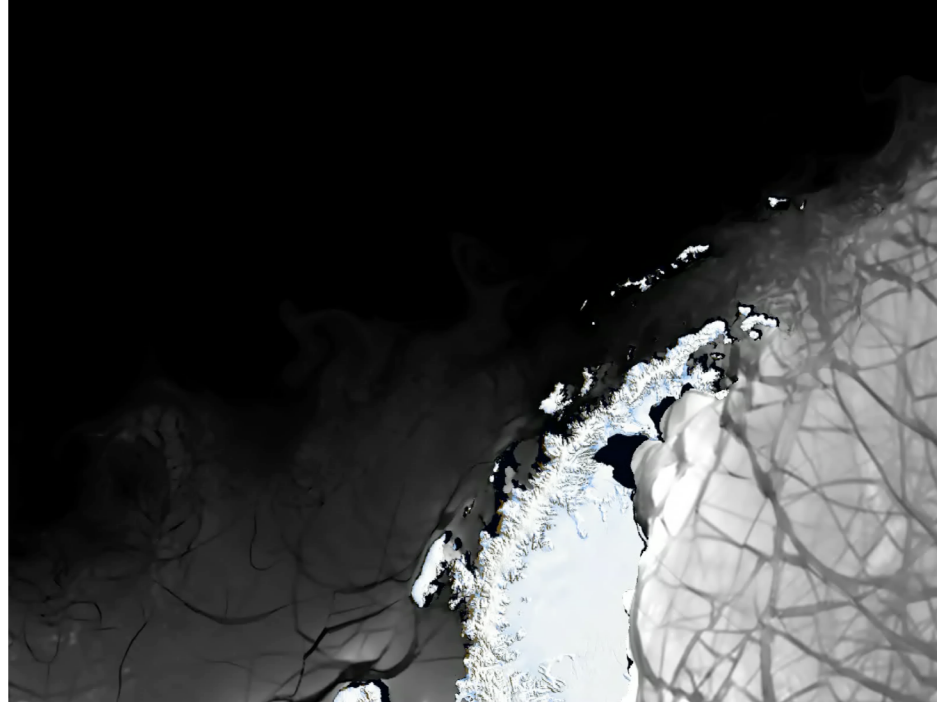
Horizontal grid spacing: 1 km

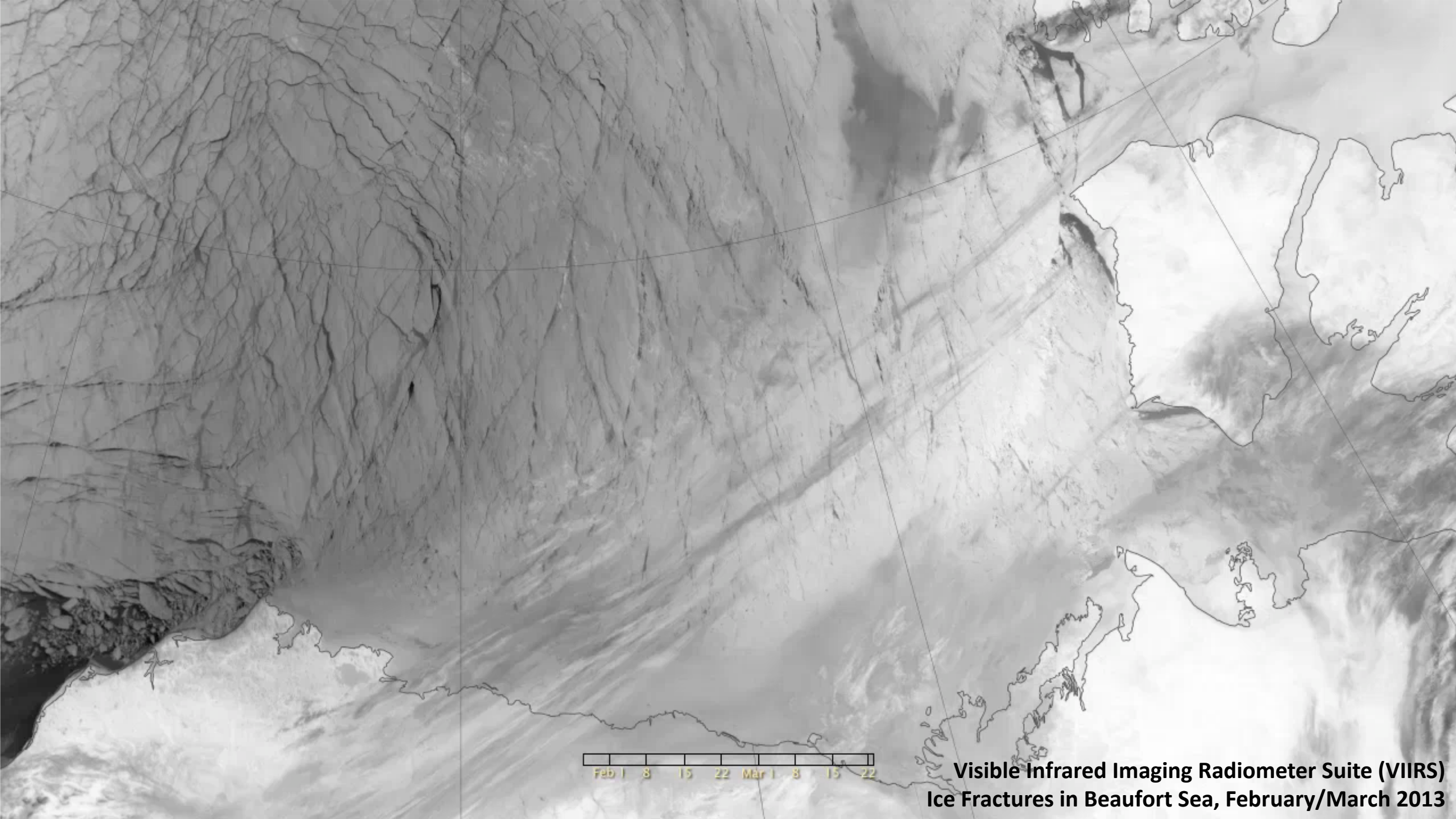


2011/09/13

(Hutter et al., 2018)



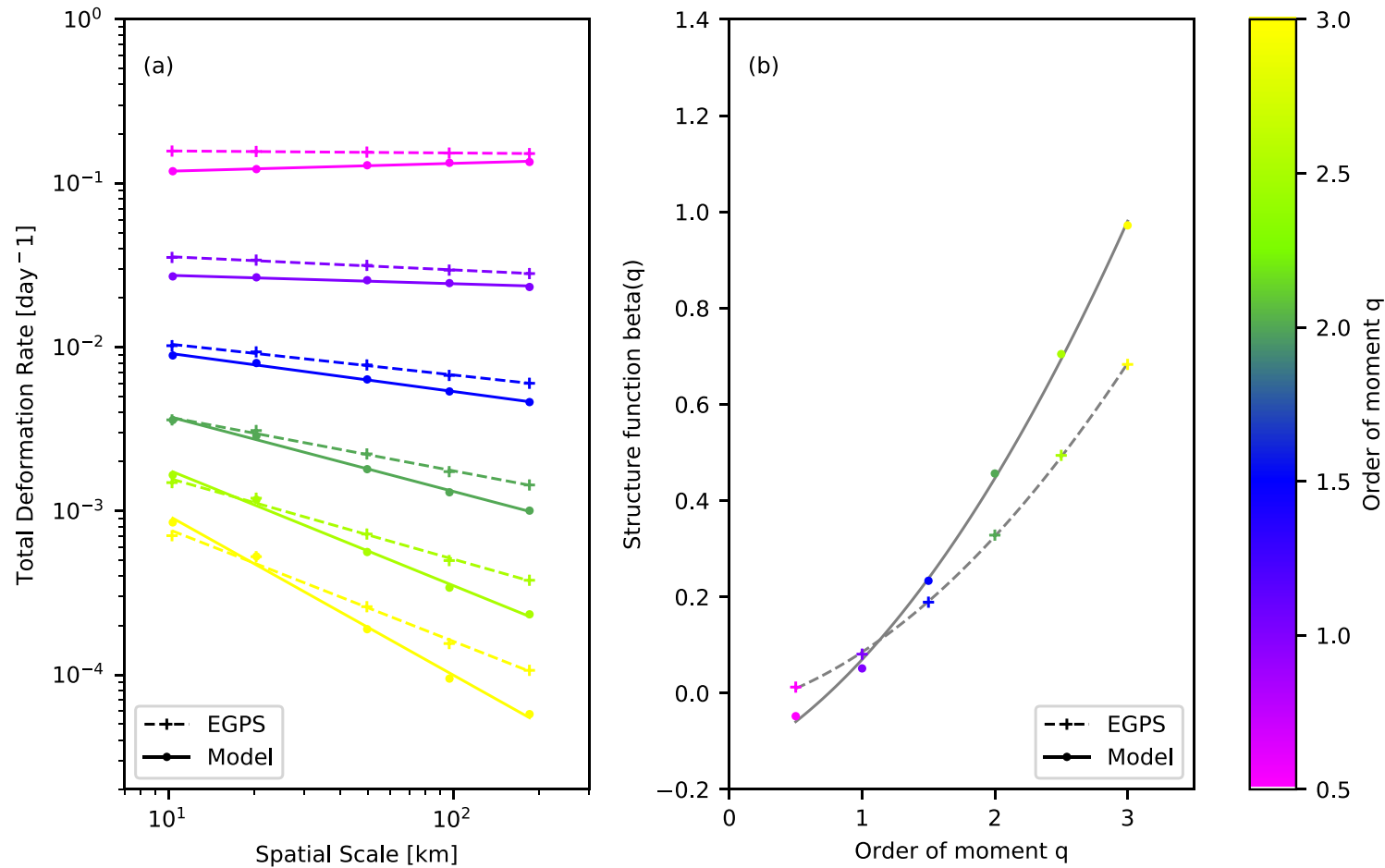




Feb 1 8 15 22 Mar 1 8 15 22

**Visible Infrared Imaging Radiometer Suite (VIIRS)  
Ice Fractures in Beaufort Sea, February/March 2013**

# Comparison of scaling properties of Arctic sea ice deformation with SAR observations (Hutter et al. 2018)



Left plot: Spatial scaling analysis for different moments for model output and EGPS data.

Right plot: Structure function computed from linear fits to left plot. The fit to a quadratic function is given in dashed (EGPS) and solid (model) lines.

The simulation reproduces observed spatial scaling of linear kinematic features (LKFs), challenging earlier studies that concluded that Viscous-plastic (VP) rheology cannot realistically represent LKFs.

The temporal scaling analysis shows that the VP model, as configured in the LLC4320 simulation, does not fully resolve the intermittency of sea ice deformation that is observed in satellite data.

# Evaluation of simulation results vs observations

- Frequency spectra at WHOI site D
- Wavenumber spectra in Drake Passage
- Comparison with glider data in Kuroshio region
- Comparison with McLane profilers
- Comparison with underway ADCP profiles in West Pacific

# Carl's notes

Comparison of LLC4320 (dashed) with WHOI site D mooring (solid) in Western North Atlantic.

Results are comparable except for the presence of the tidal overtone peaks.

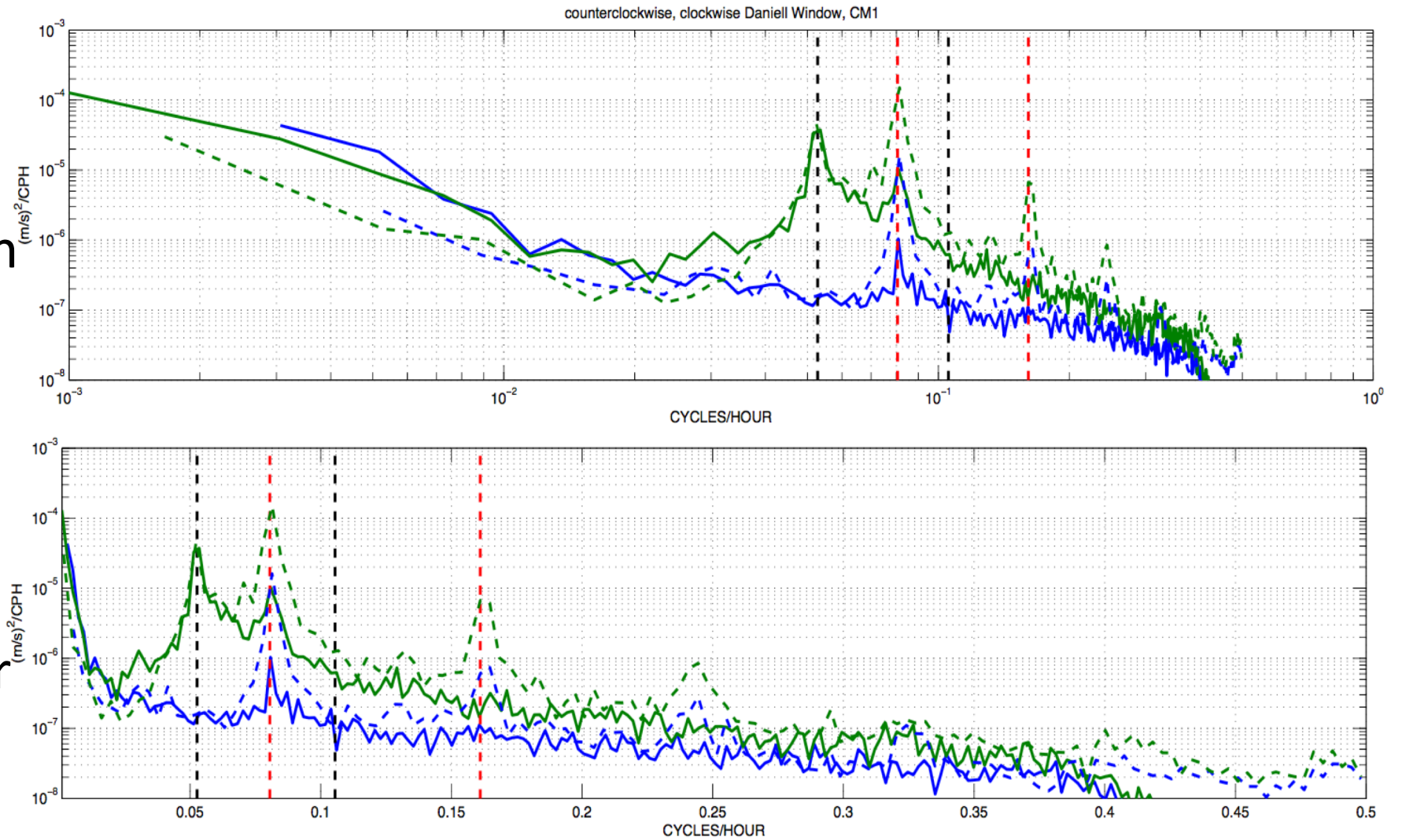


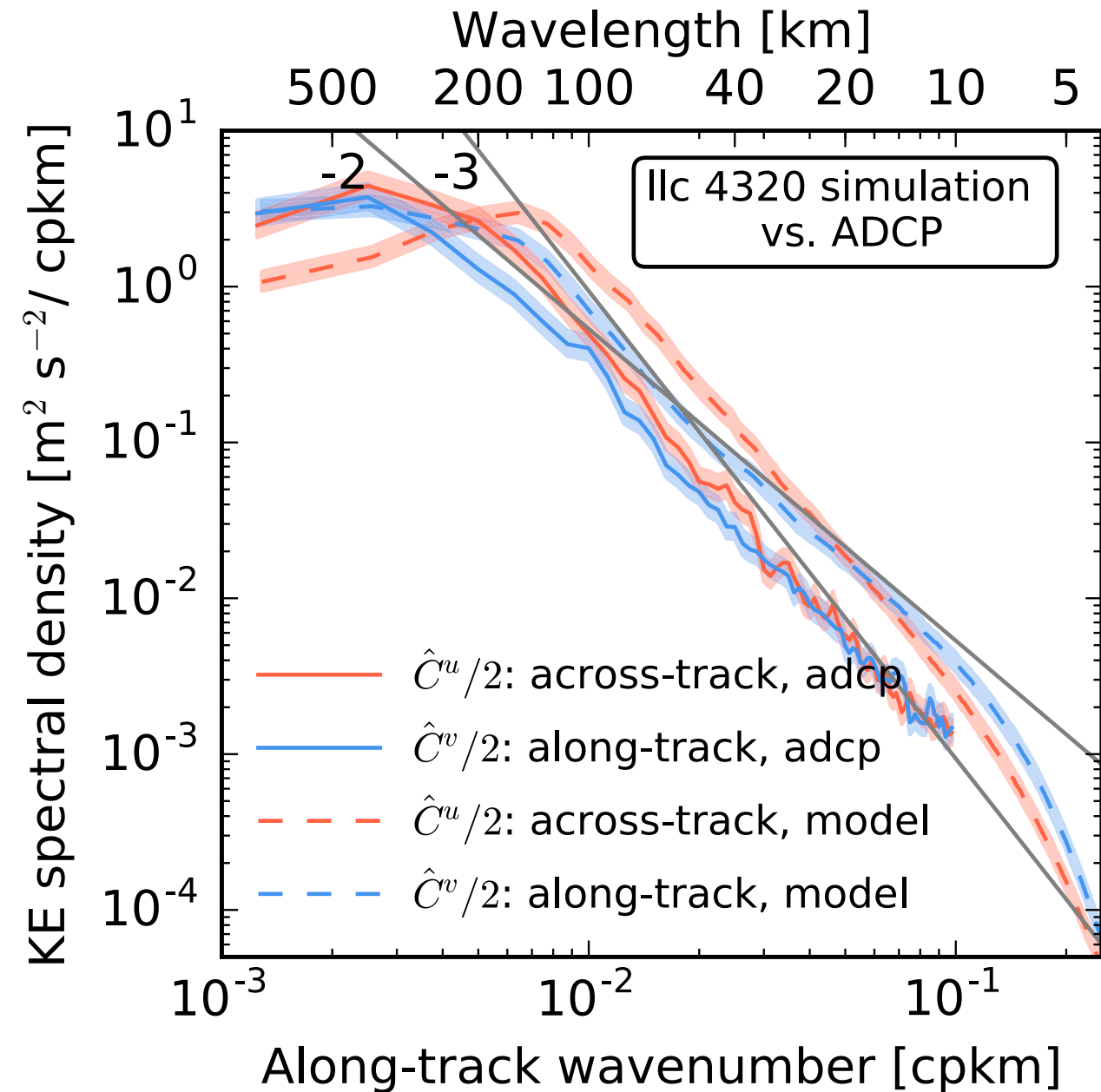
Figure 6: Rotary (clockwise, blue; counter-clockwise, green) spectra from the current meter and the model near 500m. Both logarithmic and linear displays are used. Results are comparable except, again, for the presence in the model of tidal overtone peaks and thus a generally more energetic negatively rotating spectrum.

# Mesoscale to Submesoscale Wavenumber

## Spectra in Drake Passage

(Rocha et al. 2016)

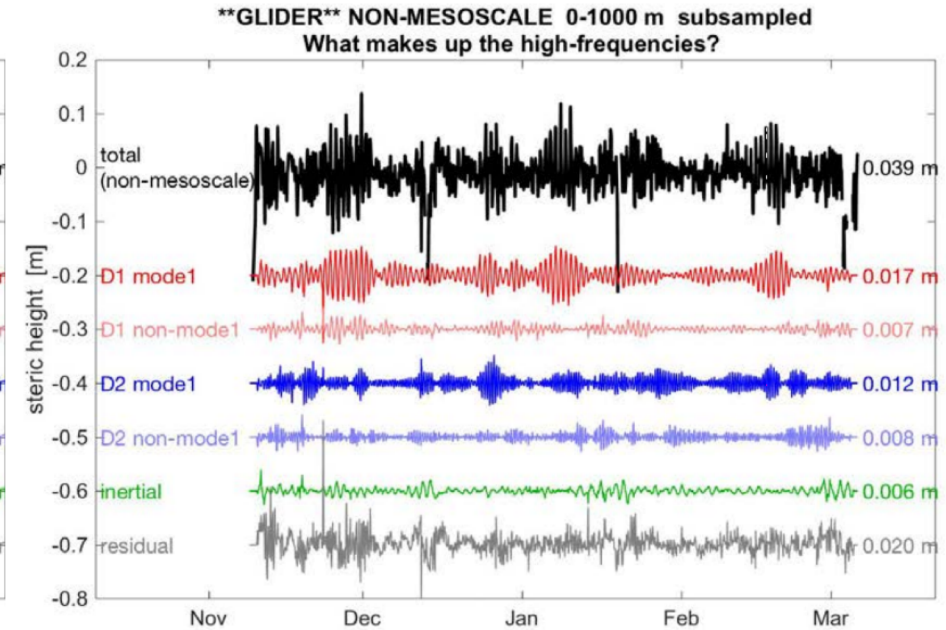
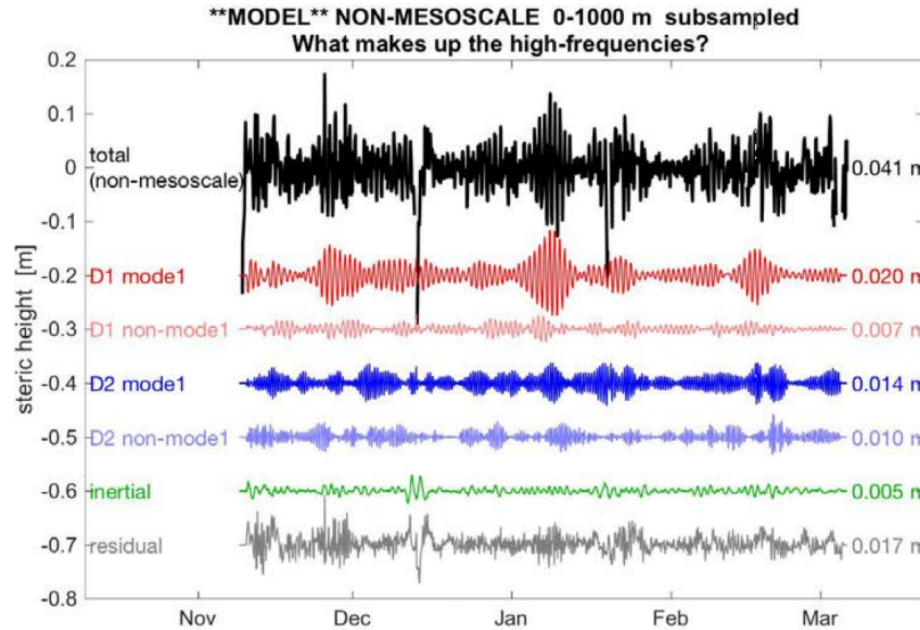
- The first three months of Ilc4320
- Inertia-gravity waves dominate scales  $<40\text{km}$  in SSH
- Compared Ilc4320 (dashed) with ADCP data (solid); gray lines are  $k^{-2}$  and  $k^{-3}$  curves.





# High frequency motions in the western Pacific

Drushka et al., 2016



## MODEL

Non-mesoscale steric height (4.1 cm)

Diurnal, mode 1	(2.0 cm)
Diurnal, non-mode1	(0.7 cm)
Semidiurnal, mode 1	(1.4 cm)
Semidiurnal, non-mode1	(1.0 cm)
Inertial motions	(0.5 cm)
Residual	(1.7 cm)

## GLIDER

Non-mesoscale steric height (3.9 cm)

Diurnal, mode 1	(1.7 cm)
Diurnal, non-mode1	(0.7 cm)
Semidiurnal, mode 1	(1.2 cm)
Semidiurnal, non-mode1	(0.8 cm)
Inertial motions	(0.6 cm)
Residual	(2.0 cm)

# High frequencies, Savage et al. 2017

LLC4320 is comparable to HYCOM25 at diurnal and semidiurnal but outperforms HYCOM25 at supertidal frequencies

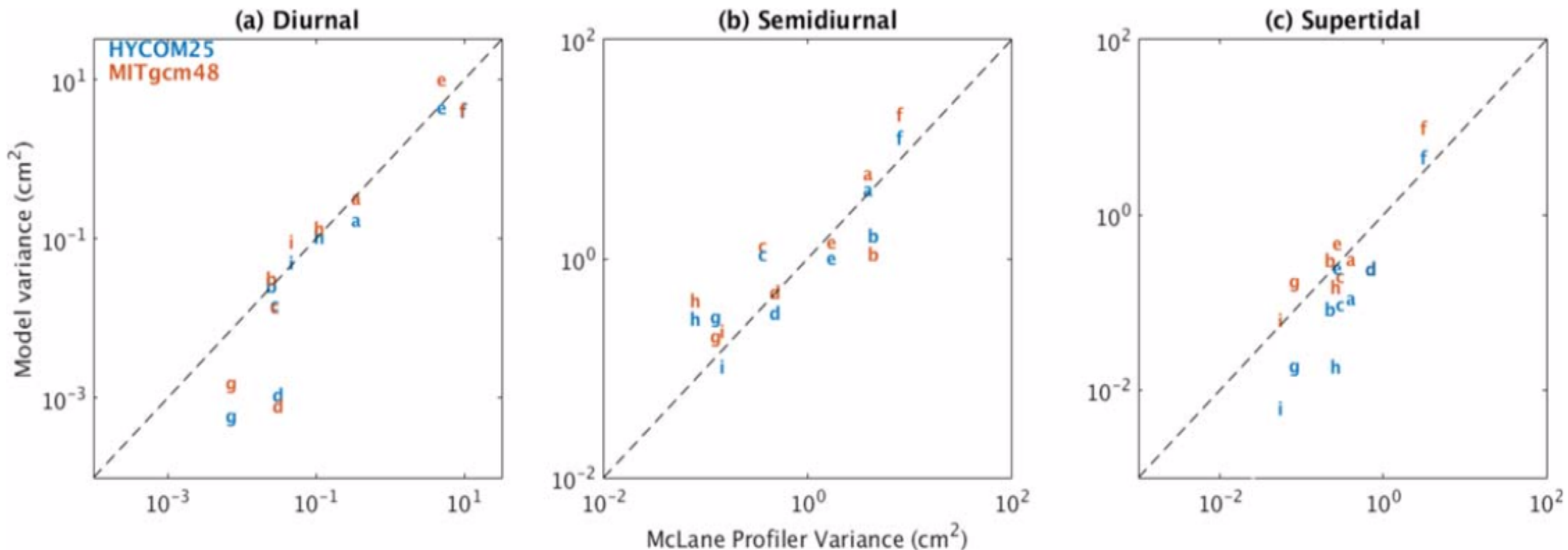
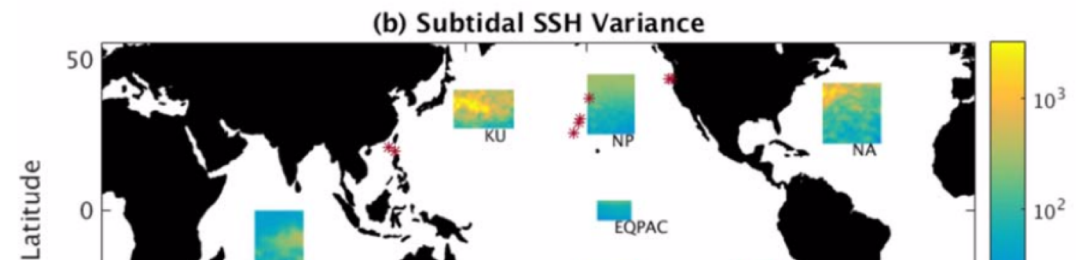


**Figure 4.** Scatterplots of band-integrated dynamic height variance vs. McLane profilers in  $1/25^\circ$  HYCOM and  $1/48^\circ$  MITgcm in (a) diurnal, (b) semidiurnal, and (c) supertidal frequency bands. Letters on scatterplots correspond to profiler locations listed in Table 1.

- ADCP data cross western pacific
- Good model-data agreement of the zonal jets structure

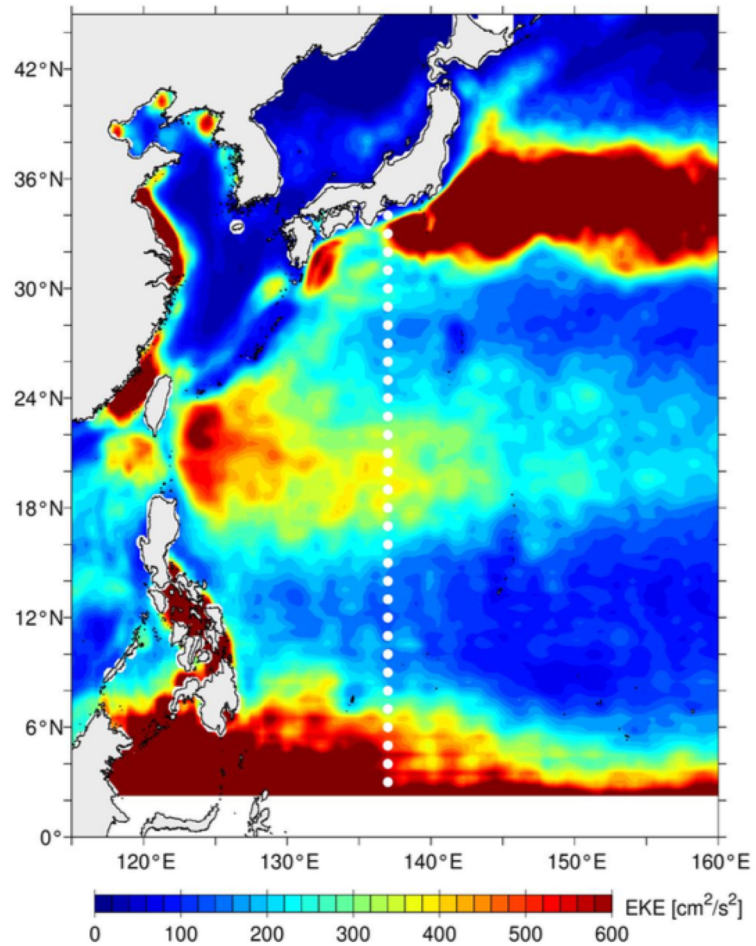


Figure 1: Surface eddy kinetic energy (EKE) distribution in the northwestern Pacific based on the weekly AVISO SSH anomaly data of 2004-2015. White dots along 137°E denote the transect of repeat ship-board ADCP measurements by Japan Meteorological Agency.

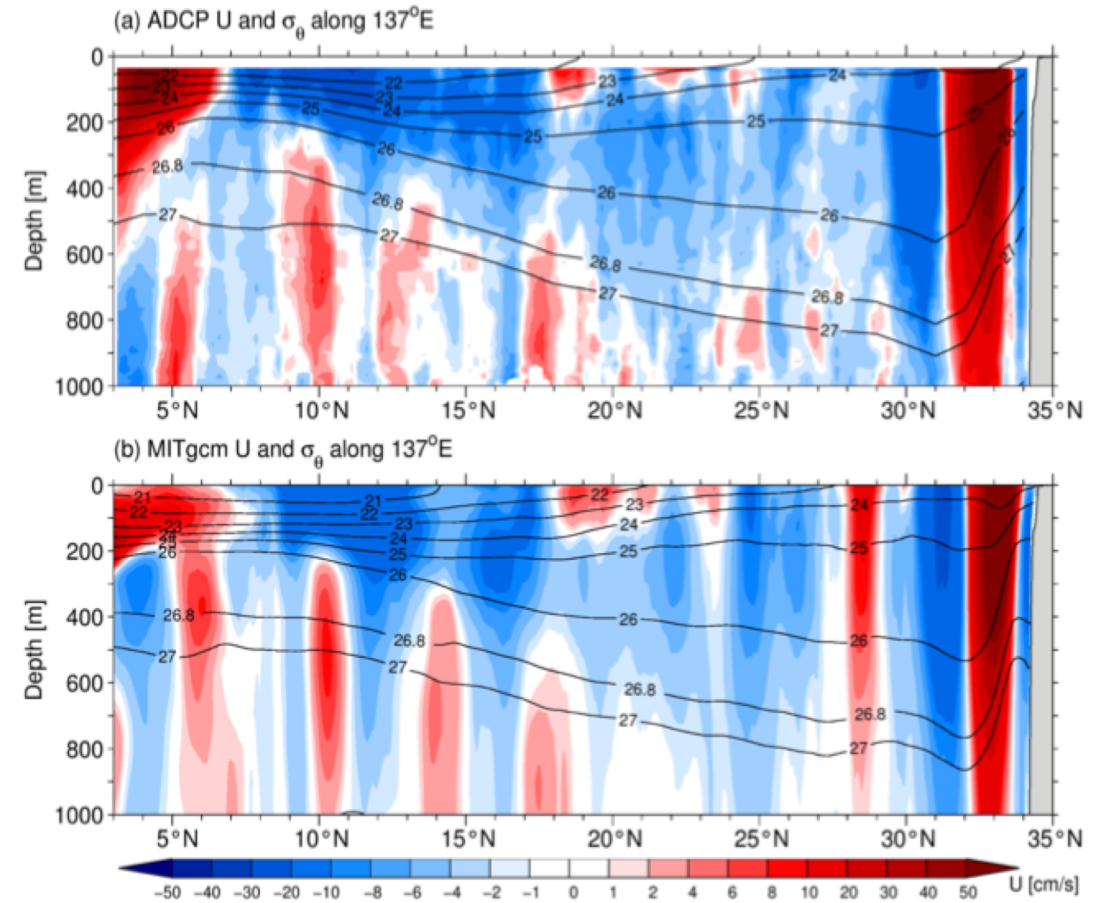
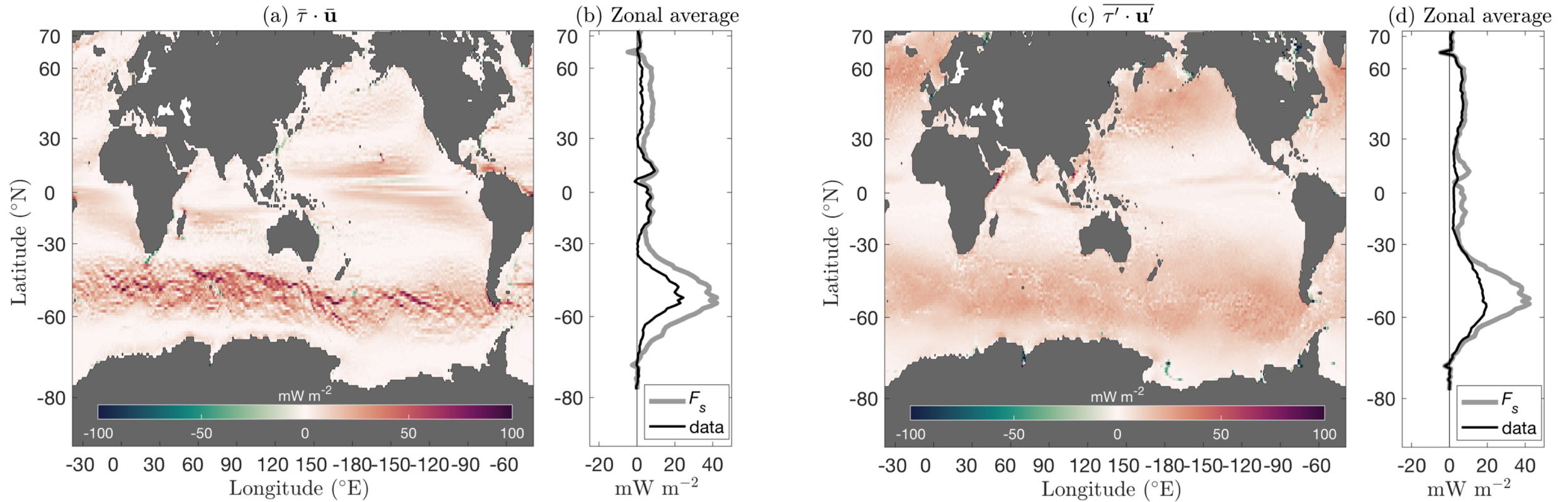


Figure 2: Latitude-depth sections of time-mean zonal velocity (colored contours) and density (black contours in  $\sigma_\theta$ ) along 137°E from (a) JMA repeat ADCP surveys of 2004-2016 and (b) MITgcm. Note that contour scales are nonlinear and red (blue) colors denote eastward (westward) flows.

# Some upper ocean applications

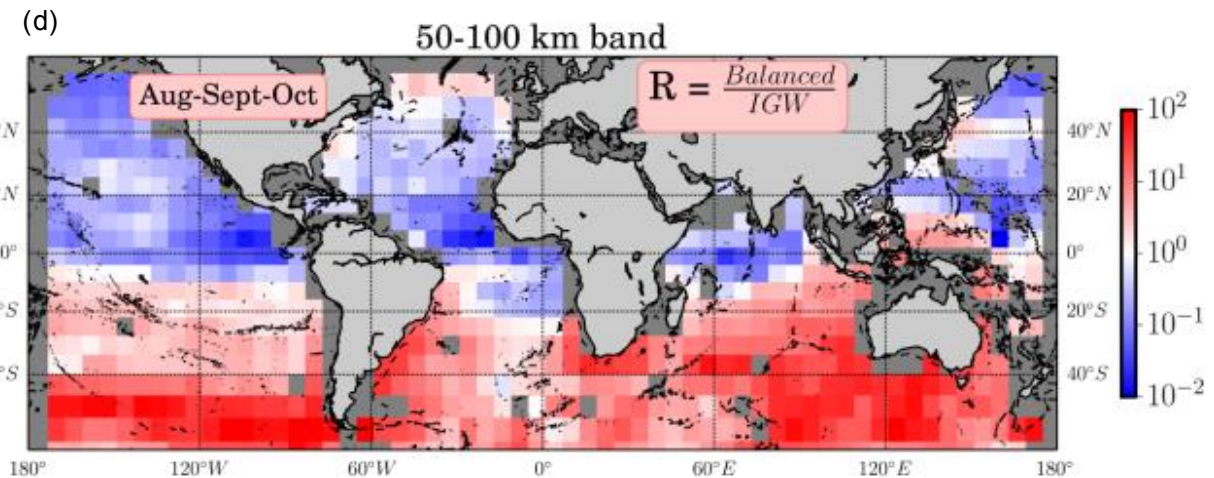
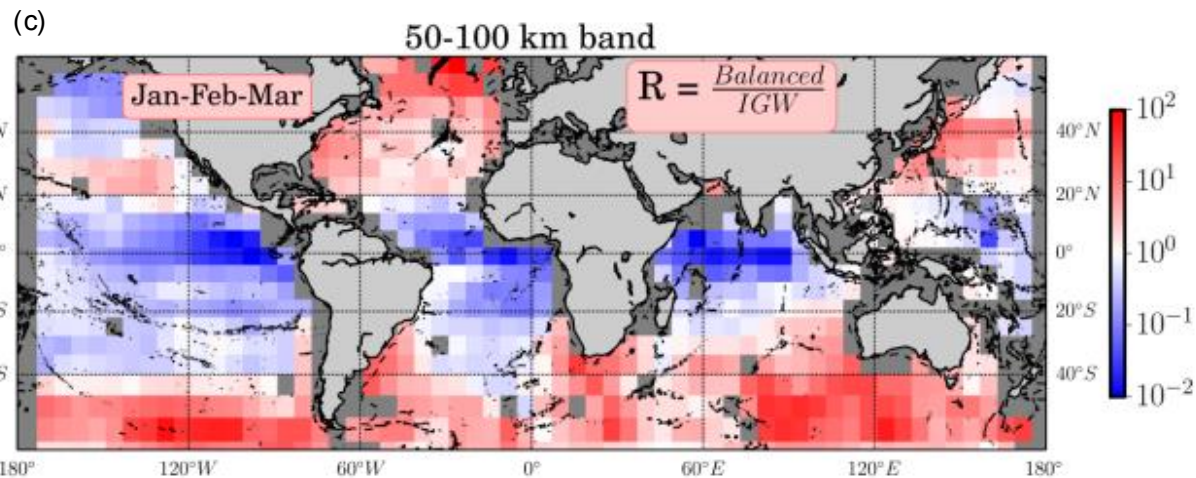
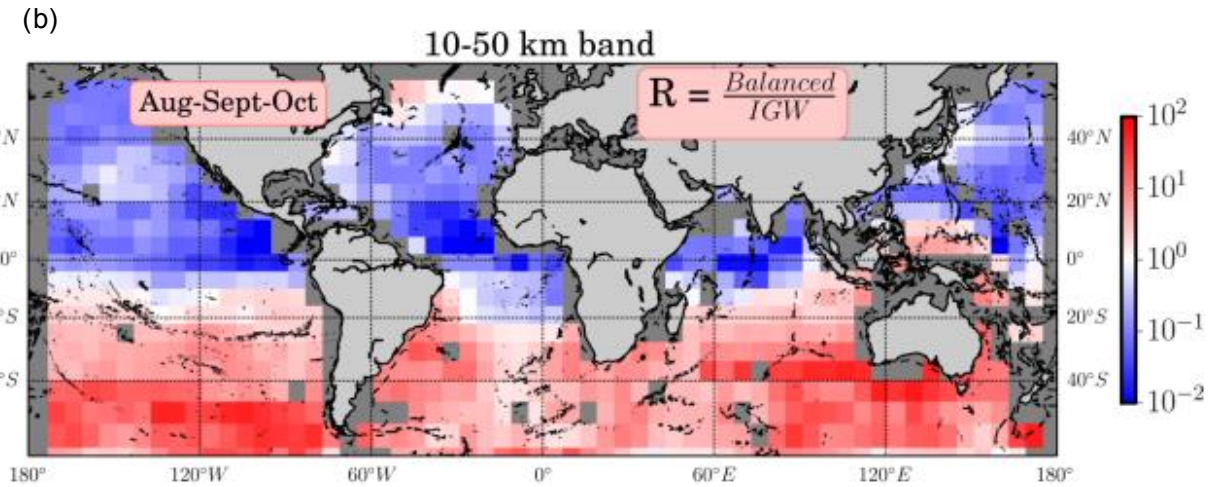
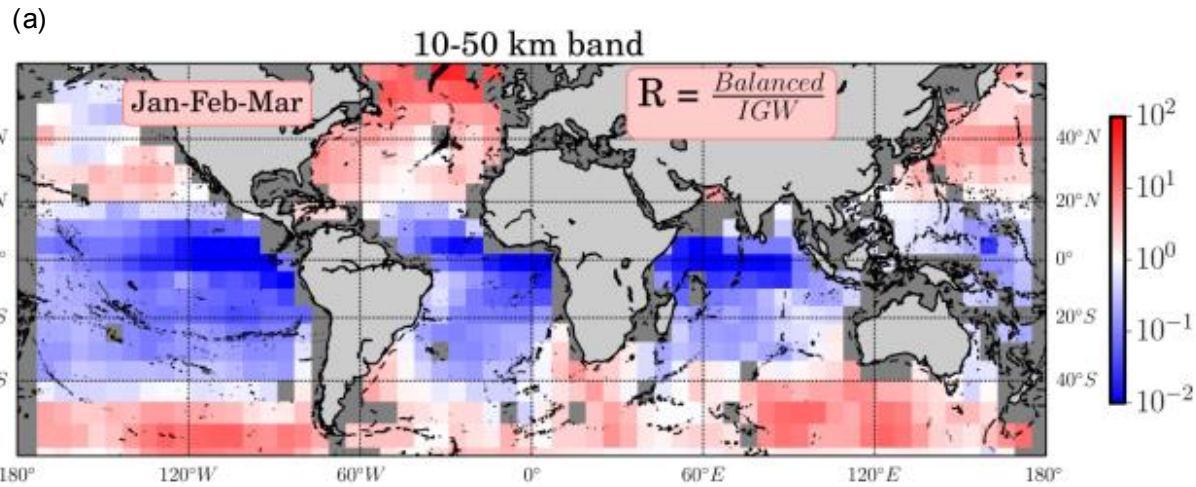
- Global estimates of surface kinetic energy fluxes
- Partitioning ocean motions into balanced and Internal Gravity Waves
- Submesoscale upward vertical heat fluxes
- Impact of including sub-daily variability on near-surface vertical fluxes

# Global estimates of surface kinetic energy fluxes caused by wind work (Flexas et al., submitted)



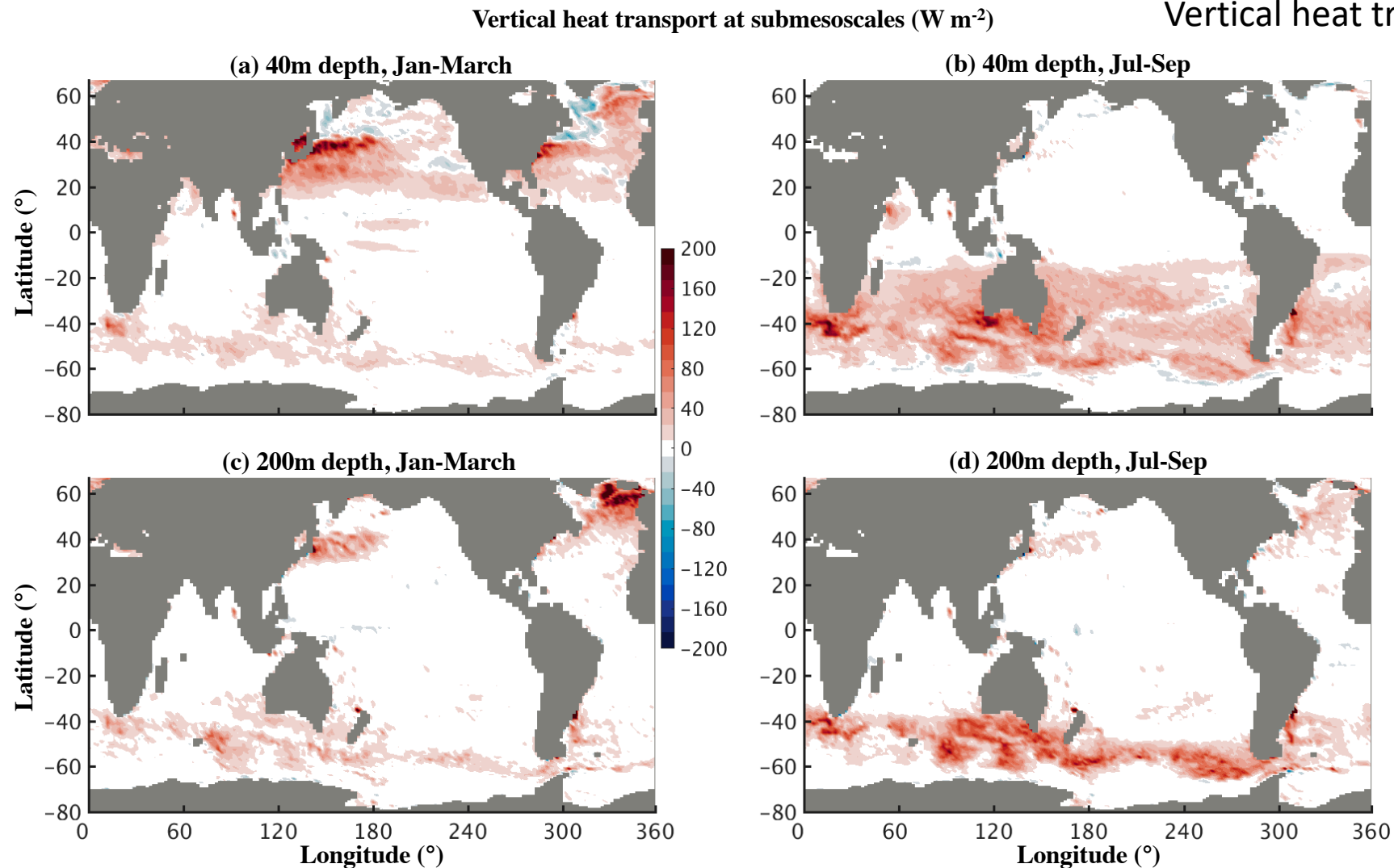
Contribution of the time-mean (left panel) and time-varying (right panel) winds and currents to the total surface energy fluxes

# Partitioning ocean motions into balanced and internal gravity waves (Torres et al., submitted)



Global maps of balanced/IGW ratio for kinetic energy for different wavelength bands and seasons.

# Strong impact of submesoscales on the (upward) vertical heat fluxes: up to 100-200 W/m<sup>2</sup> --> air-sea interactions



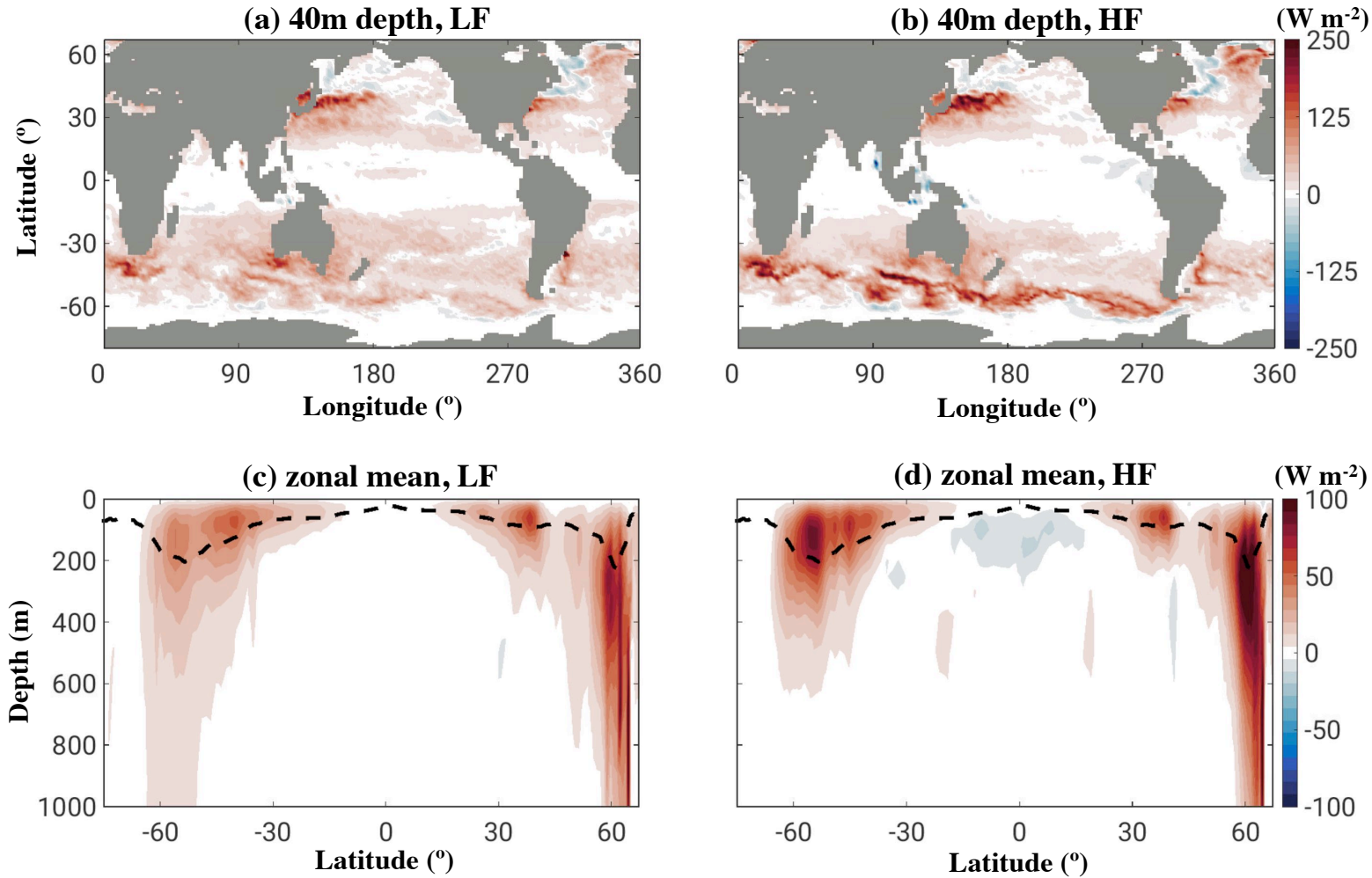
Note that vertical heat fluxes are up-gradient (not down-gradient as is often assumed in climate-model vertical mixing parameterizations).

Su et al. Nature Comm., 2018.

Global maps of the vertical heat transport in the submesoscale band [2 – 50 km] (W/m<sup>2</sup>). 20-200 W/m<sup>2</sup>.

# Sub-daily motions approx. double submesoscale vertical ocean heat fluxes (Su et al., in prep.)

## vertical heat flux (winter)



Submesoscale-range vertical heat flux at 40m depth in wintertime, calculated by daily-mean model output.

Difference of vertical heat fluxes based on hourly vs daily-mean (left column) model output.



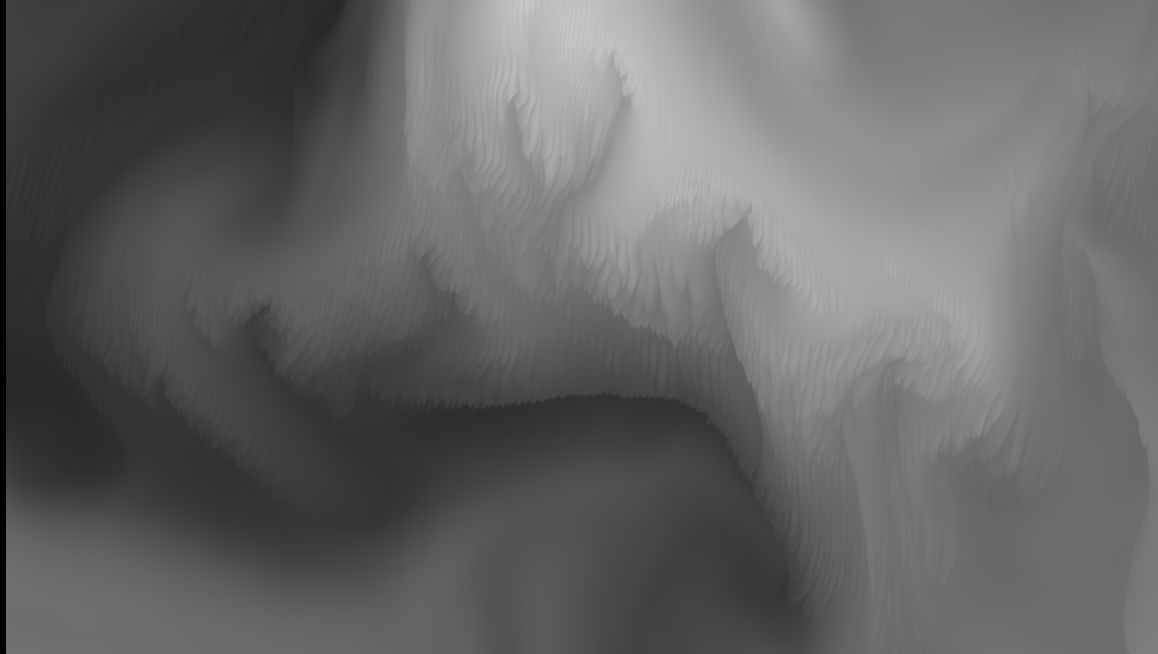
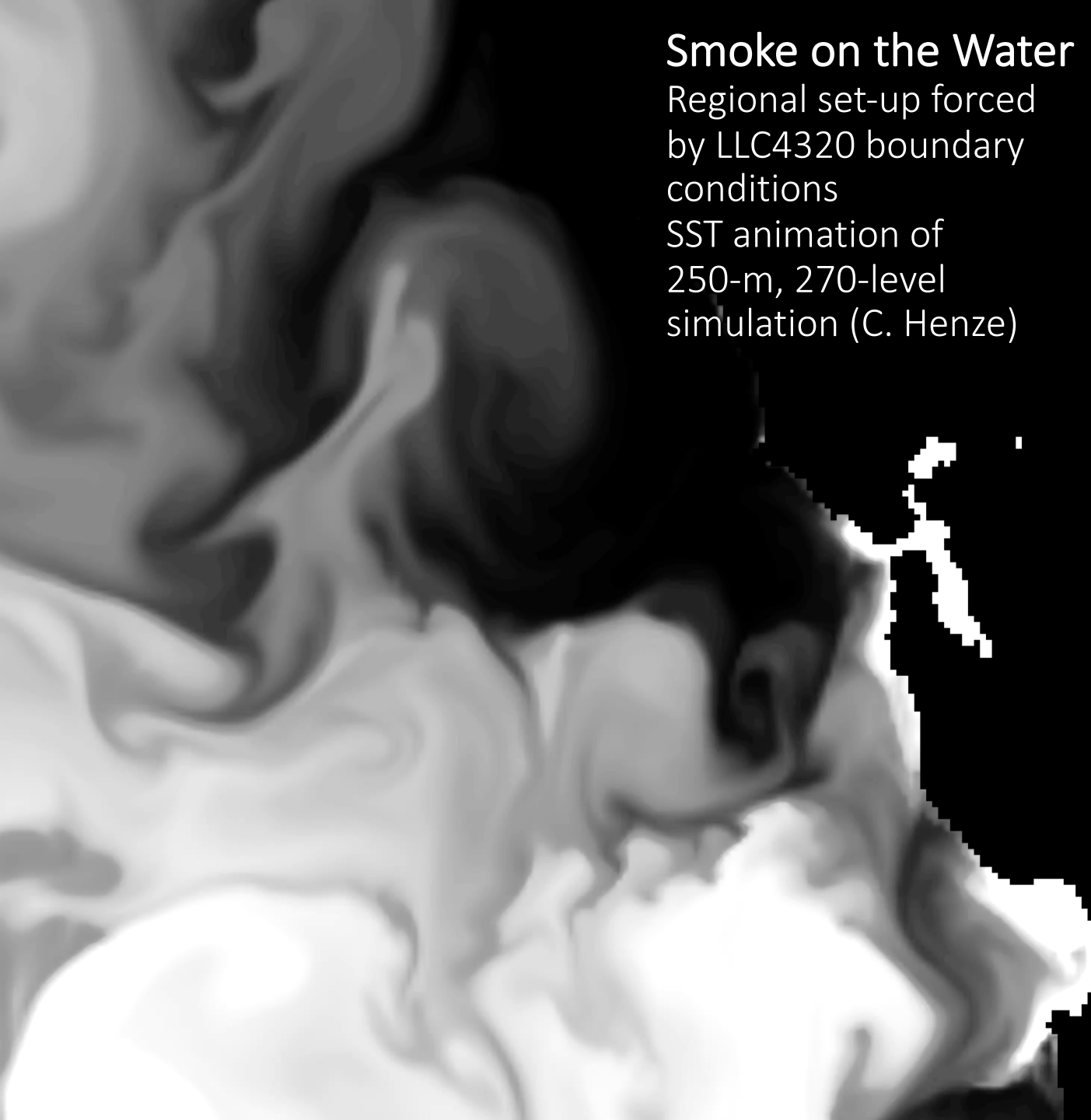
# Future directions and concluding remarks

- Higher-resolution regional simulations
- Interactive atmosphere

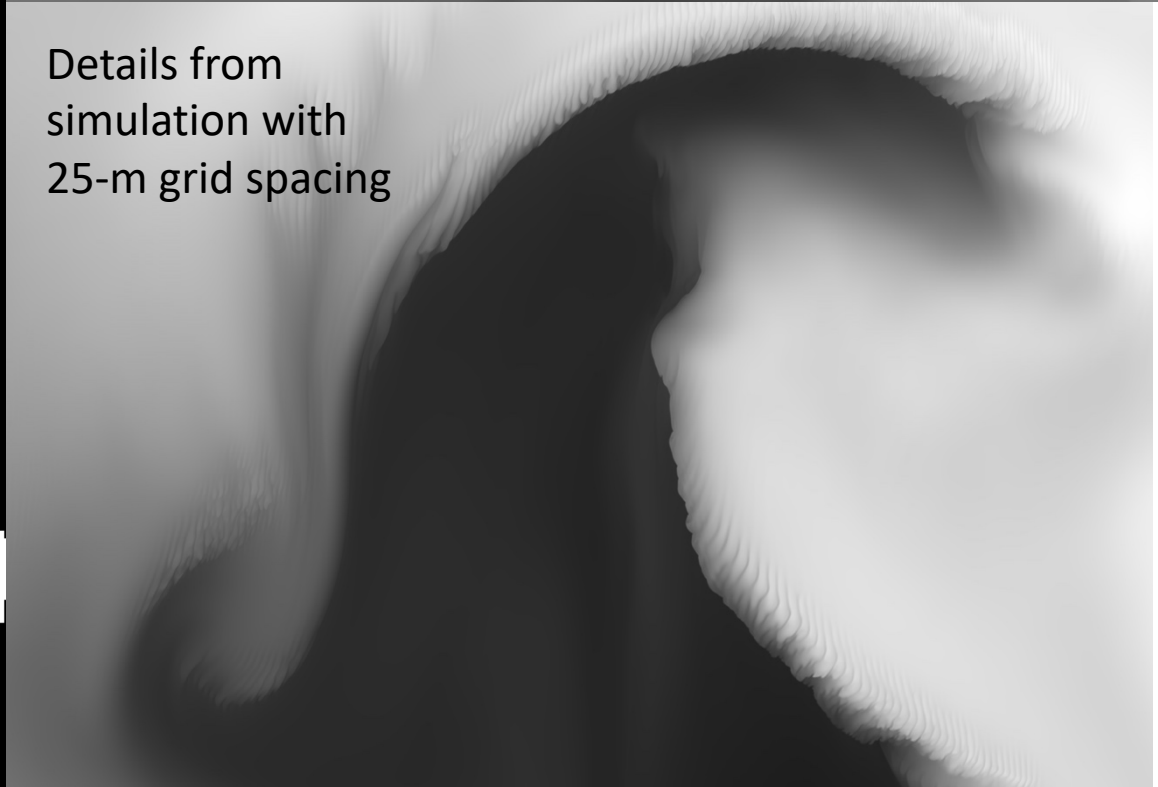
# Smoke on the Water

Regional set-up forced  
by LLC4320 boundary  
conditions

SST animation of  
250-m, 270-level  
simulation (C. Henze)



Details from  
simulation with  
25-m grid spacing

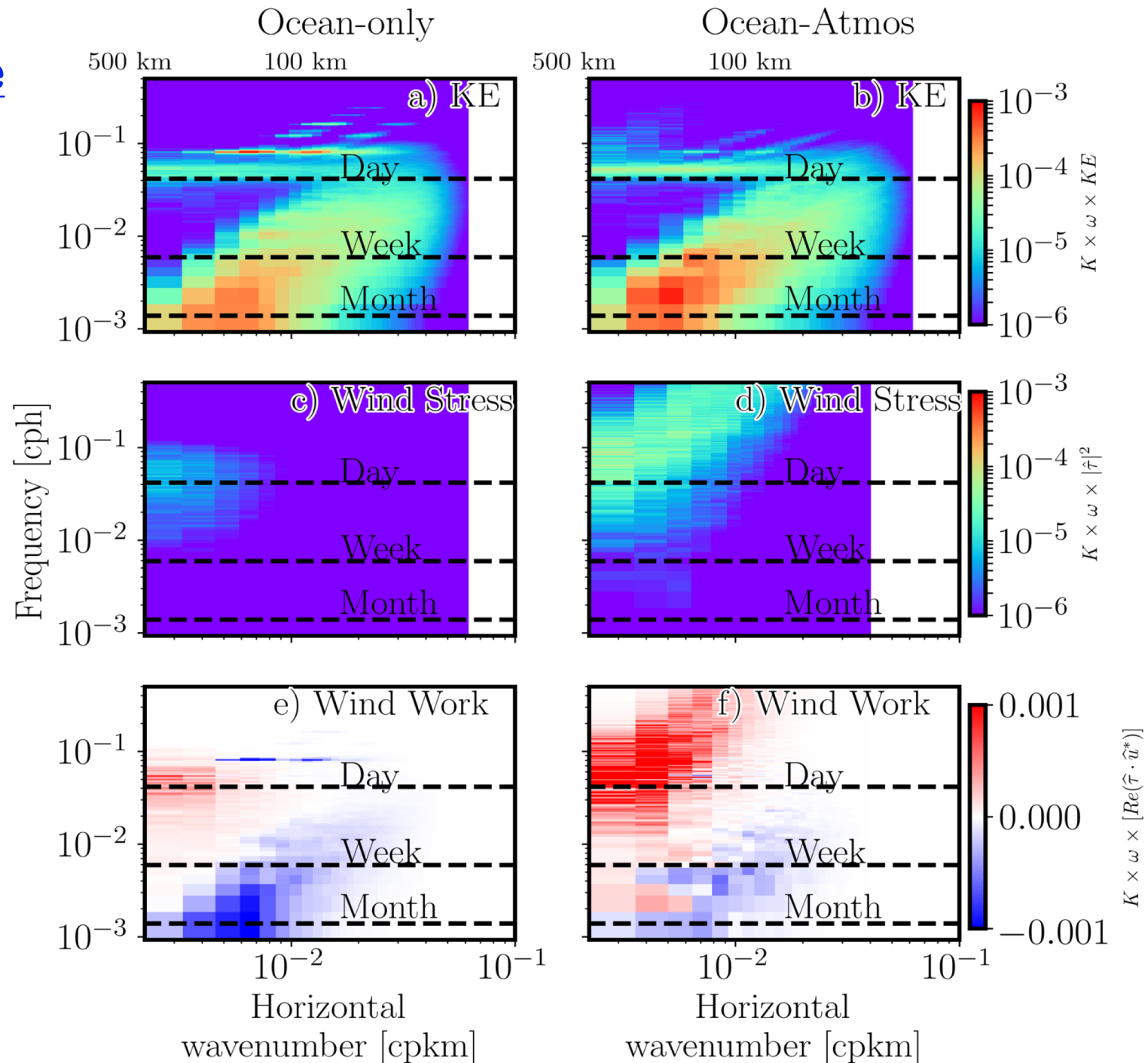


# Impact of ocean-atmosphere coupling on upper ocean

- **Top row:** surface currents
- **Middle row:** The wind stress
- **Bottom row:** Kinetic energy flux from the atmosphere to the ocean

**Surface currents, wind stress, and wind-work will be directly observed by Doppler Scatterometry missions**

**(slide by Hector Torres)**



# Concluding remarks

- Simultaneous observations of surface currents and wind stress would be a direct measurement of surface kinetic energy fluxes, which contribute to vertical mixing and large-scale ocean circulation.
- They would allow partitioning of balanced vs unbalanced (ageostrophic) surface motions, helping to further constrain upper ocean energetics.
- They would help quantify impact of near-surface vertical motions to air-sea exchanges of heat and carbon dioxide, which regulate climate and make life, as we know it, possible on this planet.